magnetochemistry

MDPI

Supplementary Material

Single-Ion Magnet and Photoluminescence Properties of Lanthanide(III) Coordination Polymers Based on Pyrimidine-4,6-Dicarboxylate

Oier Pajuelo-Corral [1], Jose Angel García [2], Oscar Castillo [3,4], Antonio Luque [3,4], Antonio Rodríguez-Diéguez [5] and Javier Cepeda [1,*]

[1] Departamento de Química Aplicada, Facultad de Química, Universidad del País Vasco/Euskal Herriko Unibertsitatea (UPV/EHU), 20018 Donostia, Spain; oier.pajuelo@ehu.eus
[2] Departamento de Física Aplicada II, Facultad de Ciencia y Tecnología, Universidad del País Vasco/Euskal Herriko Unibertsitatea (UPV/EHU), 48940 Leioa, Spain; joseangel.garcia@ehu.eus
[3] Departamento de Química Inorgánica, Facultad de Ciencia y Tecnología, Universidad del País Vasco/Euskal Herriko Unibertsitatea (UPV/EHU), 48940 Leioa, Spain; oscar.castillo@ehu.eus (O.C.); antonio.luque@ehu.eus (A.L.)
[4] BCMaterials, Basque Center for Materials, Applications and Nanostructures, UPV/EHU Science Park, 48940 Leioa, Spain
[5] Departamento de Química Inorgánica, Facultad de Ciencias, Universidad de Granada, 18071 Granada, Spain; antonio5@ugr.es
* Correspondence: javier.cepeda@ehu.es; Tel.: +34-943015409

Contents:

Citation: Pajuelo-Corral, O.; Garc, J.A.; Castillo, O.; Luque, A.; Rodr, A.; Cepeda, J. Single-Ion Magnet and Photoluminescence Properties of Lanthanide(III) Coordination Polymers Based on Pyrimidine-4,6-dicarboxylate. *Magnetochemistry* **2021**, *7*, 8. https://doi.org/10.3390/magnetochemistry7010008

Received: 4 December 2020
Accepted: 29 December 2020
Published: 4 January 2021

S1. Elemental analysis

Compound 1-Dy: Anal. Calc. for $C_7H_{12}DyN_2O_{11}$ (%): C, 18.17; H, 2.61; N, 6.05. Found (%): C, 18.25; H, 2.48; N, 6.21. Yield 65-70% based on metal.

Compound 2-Dy: Anal. Calc. for $C_7H_{10.66}DyN_2O_{10.33}$ (%): C, 18.66; H, 2.38; N, 6.22. Found (%): C, 18.49; H, 2.26; N, 6.31. Yield 65-70% based on metal.

Compound 3-Dy: Anal. Calc. for $C_{14}H_{20}Dy_2N_4O_{20}$ (%): C, 18.91; H, 2.27; N, 6.30. Found (%): C, 18.78; H, 2.12; N, 6.43. Yield 55-60% based on metal.

Compound 4-Nd: Anal. Calc. for $C_7H_8N_2NdO_9$ (%): C, 20.59; H, 1.97; N, 6.86. Found (%): C, 20.67; H, 2.11; N, 6.70. Yield 70-75% based on metal.

Compound 4-Sm: Anal. Calc. for $C_7H_8N_2SmO_9$ (%): C, 20.28; H, 1.95; N, 6.76. Found (%): C, 20.15; H, 2.08; N, 6.91. Yield 45-50% based on metal.

Compound 4-Eu: Anal. Calc. for $C_7H_8N_2EuO_9$ (%): C, 20.21; H, 1.94; N, 6.73. Found (%): C, 20.33; H, 1.90; N, 6.88. Yield 50-55% based on metal.

Compound 4-Dy: Anal. Calc. for $C_7H_8N_2DyO_9$ (%): C, 19.71; H, 1.89; N, 6.57. Found (%): C, 19.68; H, 1.98; N, 6.42. Yield 60-65% based on metal.

Compound 5-Dy: Anal. Calc. for $C_6H_6DyN_3O_9$ (%): C, 16.89; H, 1.42; N, 9.85. Found (%): C, 16.72; H, 1.65; N, 9.82. Yield 80-85% based on metal.

S2. Powder X-ray diffraction analysis.

The Dy-based compounds have been analyzed by PXRD as shown in Figure S3.

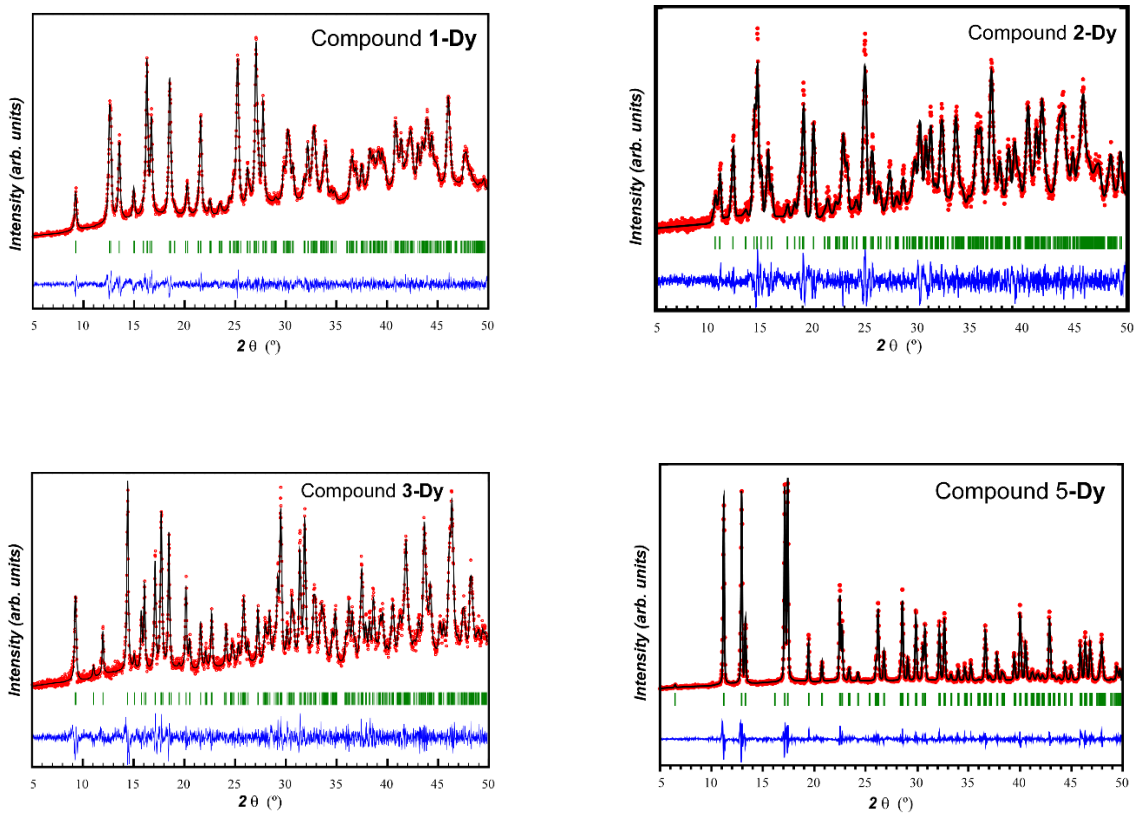

Figure S1. Pattern-matching analyses on the diffractograms of previously reported Dy-based compounds.

In the following figure, all the pattern matching analysis of the novel compounds are gathered.

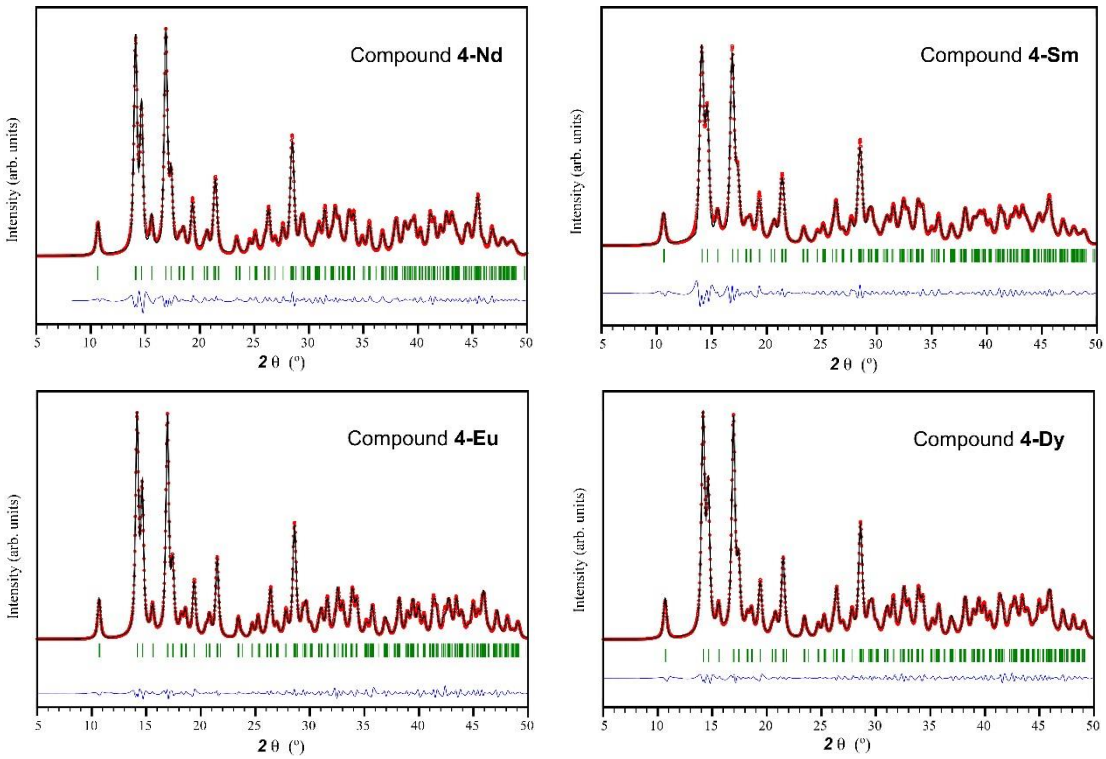

Figure S2. Full profile pattern-matching analyses performed on the diffractograms of **4-Nd, 4Sm, 4-Eu** and **4-Dy**.

S3. Crystallographic data

Table S1. Crystallographic data for compounds **4-Nd**, **4-Sm** and **4-Eu**.

	4-Nd	**4-Sm**	**4-Eus**
Empirical formula	C7H8N2NdO9	C7H8N2SmO9	C7H8EuN2O9
Formula weight	408.39	414.50	416.11
Crystal system	monoclinic	monoclinic	monoclinic
Space group	$P2_1/n$	$P2_1/n$	$P2_1/n$
a (Å)	6.8700(3)	6.8540(2)	6.8390(5)
b (Å)	16.6840(6)	16.5860(5)	16.4870(9)
c (Å)	9.7030(3)	9.6750(3)	9.6400(5)
β/ °	100.289(4)	100.425(3)	100.436(6)
V (Å^3)	1094.26(7)	1081.70(6)	1068.97(11)
Z	4	4	4
Reflections collected	6868	8230	6880
Unique data/parameters	2249/172	3504/173	2200/172
Rint	0.0318	0.0453	0.0567
GoF (S)[a]	1.044	1.038	1.026
R1[b]/wR2[c] [I>2σ(I)]	0.0300/0.0776	0.0492/0.1314	0.0332/0.0686
R1[b]/wR2[c] [all]	0.0325/0.0797	0.0531/0.01345	0.0448/0.0710

[a] $S = [\sum w(F_0^2 - F_c^2)^2 / (N_{obs} - N_{param})]^{1/2}$. [b] $R_1 = \sum ||F_0| - |F_c|| / \sum |F_0|$; [c] $wR^2 = [\sum w(F_0^2 - F_c^2)^2 / \sum wF_0^2]^{1/2}$; $w = 1/[\sigma^2(F_0^2) + (aP)^2 + bP]$ where $P = (\max(F_0^2,0) + 2F_c^2)/3$ with a = 0.0542 (**4-Nd**), 0.1131 (**4-Sm**), 0.0341 (**4-Eu**) and b = 0.1440 (**4-Nd**), 0.0000 (**4-Sm**), 1.4422 (4-Eu).

S4. Structural details of compounds.

Table S2. CShMs for the coordination environment of compounds **1-Dy, 2-Dy, 3-Gd, 4-Nd, 4-Sm, 4-Eu** and **5-Gd**. The lowest SHAPE values for each ion are shown highlighted indicating best fits. Codes.

EP-9	1 D9h	Enneagon
OPY-9	2 C8v	Octagonal pyramid
HBPY-9	3 D7h	Heptagonal bipyramid
JTC-9	4 C3v	Johnson triangular cupola J3
JCCU-9	5 C4v	Capped cube J8
CCU-9	6 C4v	Spherical-relaxed capped cube
JCSAPR-9	7 C4v	Capped square antiprism J10
CSAPR-9	8 C4v	Spherical capped square antiprism
JTCTPR-9	9 D3h	Tricapped trigonal prims J51
TCTPR-9	10 D3h	Spherical tricapped trigonal prism
JTDIC-9	11 C3v	Tridiminished icosahedron J63
HH-9	12 C2v	Hula-hoop
MFF-9	13 Cs	Muffin

Structure [ML9]	JCSAPR-9	CSAPR-9	JTCTPR-9	TCTPR-9	MFF-9
1-Dy	1.345	**0.806**	1.679	1.126	1.122
2-Dy	2.086	0.828	2.934	**0.738**	1.041
3-Gd (Gd1)	2.469	1.367	3.974	**1.074**	1.266
3-Gd (Gd2)	0.995	**0.587**	2.666	1.367	0.802
4-Nd	1.439	**0.955**	2.952	1.701	1.011
4-Sm	1.337	**0.889**	2.913	1.589	0.993
4-Eu	1.296	**0.845**	2.928	1.571	0.955
5-Gd	1.673	0.920	3.502	2.143	**0.410**

Table S3. Selected bond lengths (Å) for compounds **1-Dy, 2-Dy, 4-Nd**, **4-Sm** and **4-Eu**[1].

Compound 1-Dy			
Dy1-N11	**2.674(3)**	**Dy1-O181 (i)**	2.398(2)
Dy1-N13 (i)	2.656(3)	Dy1-O1W	2.493(2)
Dy1-O21	2.375(2)	Dy1-O2W	2.373(2)
Dy1-O23 (ii)	2.361(2)	Dy1-O3W	2.407(2)
Dy1-O171	2.283(2)		
Compound **2-Dy**			
Dy1-N11	2.588(9)	Dy1-O181 (iii)	2.427(6)
Dy1-N13 (iii)	2.629(8)	Dy1-O182 (v)	2.361(7)
Dy1-O21	2.415(6)	Dy1-O1W	2.431(7)
Dy1-O23 (iv)	2.410(7)	Dy1-O2W	2.395(6)
Dy1-O171	2.373(6)		
Compound **4-Nd**			
Nd1-N11	2.737(3)	Nd1-O181 (vi)	2.470(3)
Nd1-N13 (vi)	2.723(3)	Nd1-O182 (viii)	2.458(3)
Nd1-O21	2.454(3)	Nd1-O1W	2.467(3)
Nd1-O23 (vii)	2.478(3)	Nd1-O2W	2.475(3)
Nd1-O171	2.407(3)		
Compound **4-Sm**			
Sm1-N11	2.724(6)	Sm1-O181 (vi)	2.441(5)
Sm1-N13 (vi)	2.697 (6)	Sm1-O182 (viii)	2.430(5)
Sm1-O21	2.427(5)	Sm1-O1W	2.431(5)
Sm1-O23 (vii)	2.453(5)	Sm1-O2W	2.456(4)
Sm1-O171	2.382(5)		
Compound **4-Eu**			
Eu1-N11	2.703(5)	Eu1-O181 (vi)	2.428(4)
Eu1-N13 (vi)	2.676 (5)	Eu1-O182 (viii)	2.432(4)
Eu1-O21	2.413(4)	Eu1-O1W	2.414(4)
Eu1-O23 (vii)	2.442 (4)	Eu1-O2W	2.446(4)
Eu1-O171	2.372(4)		

[1]Symmetry codes: (i) 1/2-x, 1/2+y, 1/2-z.; (ii) -x, -y, -z; (iii) 1/2+x, -3/2-y, z; (iv) 1+x, y, z; (v) 2-x, 1-y, -z. (vi) 1/2+x, 1/2-y, -1/2+z.; (vii) -x+1, -y, -z; (viii) x, y, -1+z.

S5 Ac magnetic susceptibility measurements.

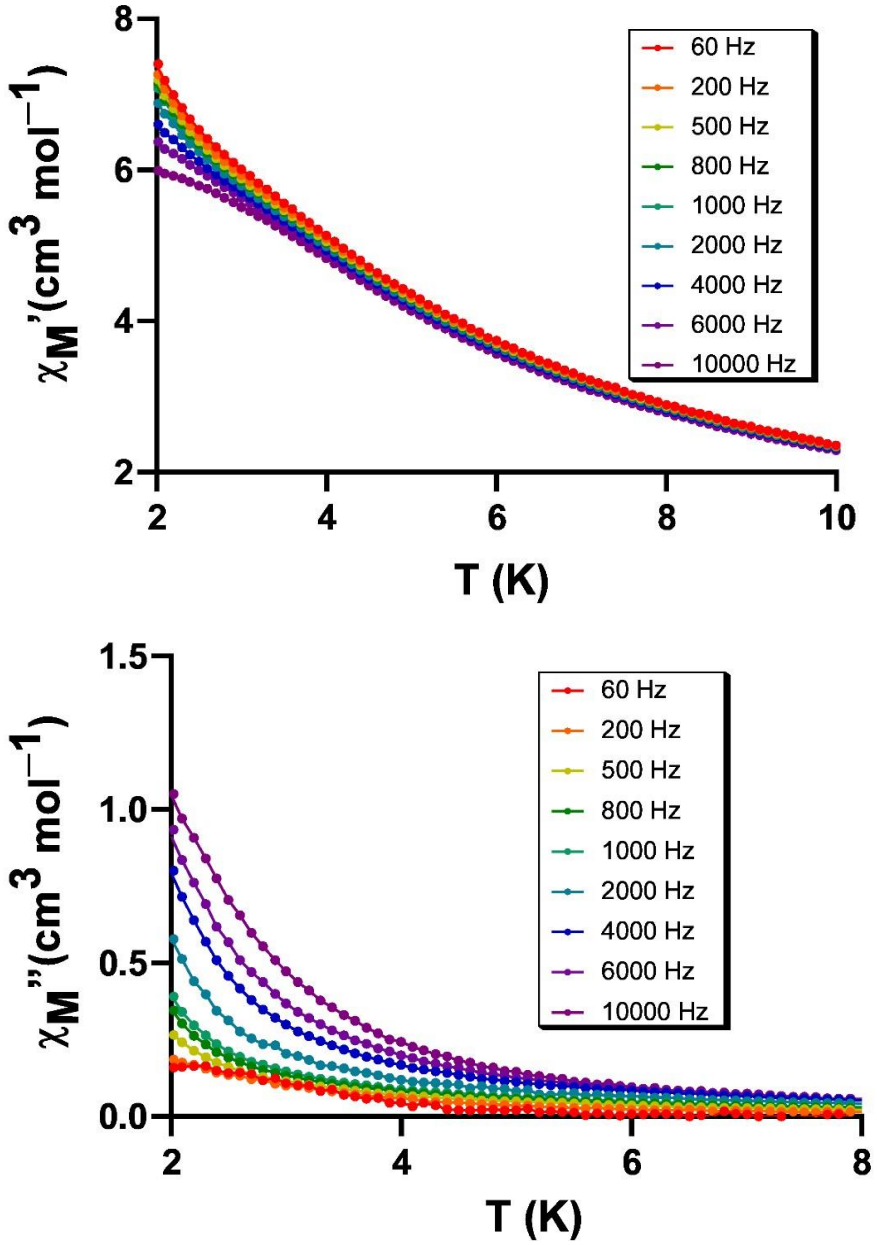

Figure S3. $\chi_M'(T)$ (top) and $\chi_M''(T)$ (bottom) signals plots for compound **3-Dy** under H_{dc} = 1000 Oe.

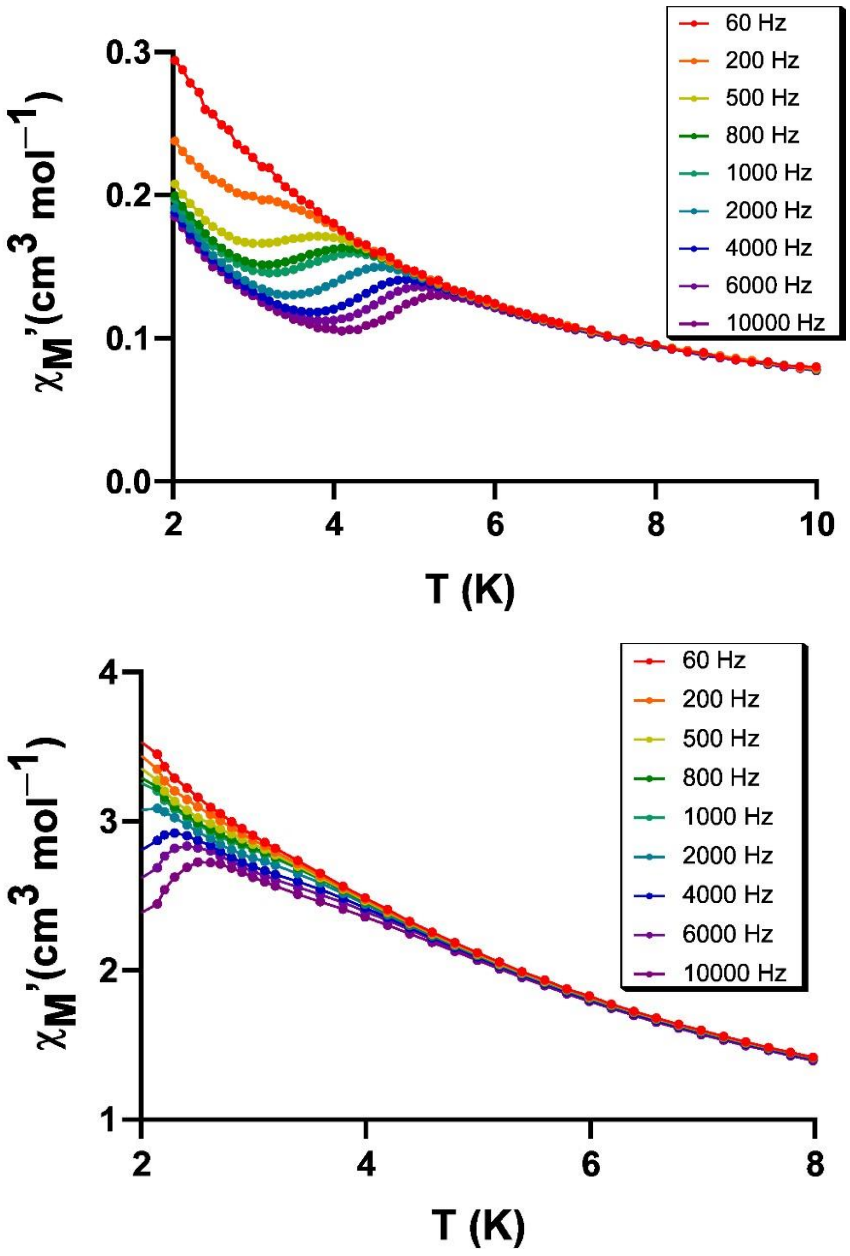

Figure S4. Temperature dependence of in-phase components of the *ac* susceptibility in a *dc* applied field of 1000 Oe for **1-Dy** (top) and **2-Dy** (bottom).

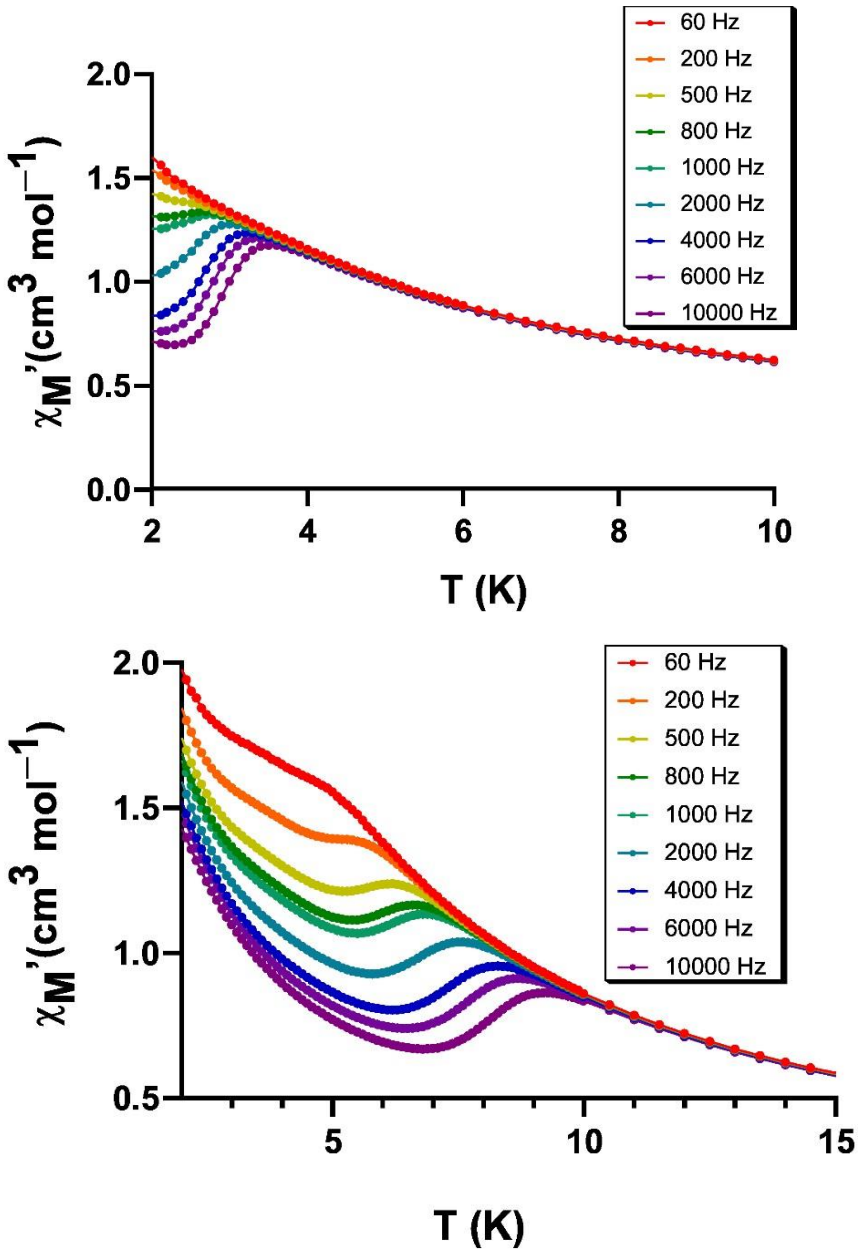

Figure S5. Temperature dependence of in-phase components of the *ac* susceptibility in a *dc* applied field of 1000 Oe for **4-Dy** (top) and **5-Dy** (bottom).

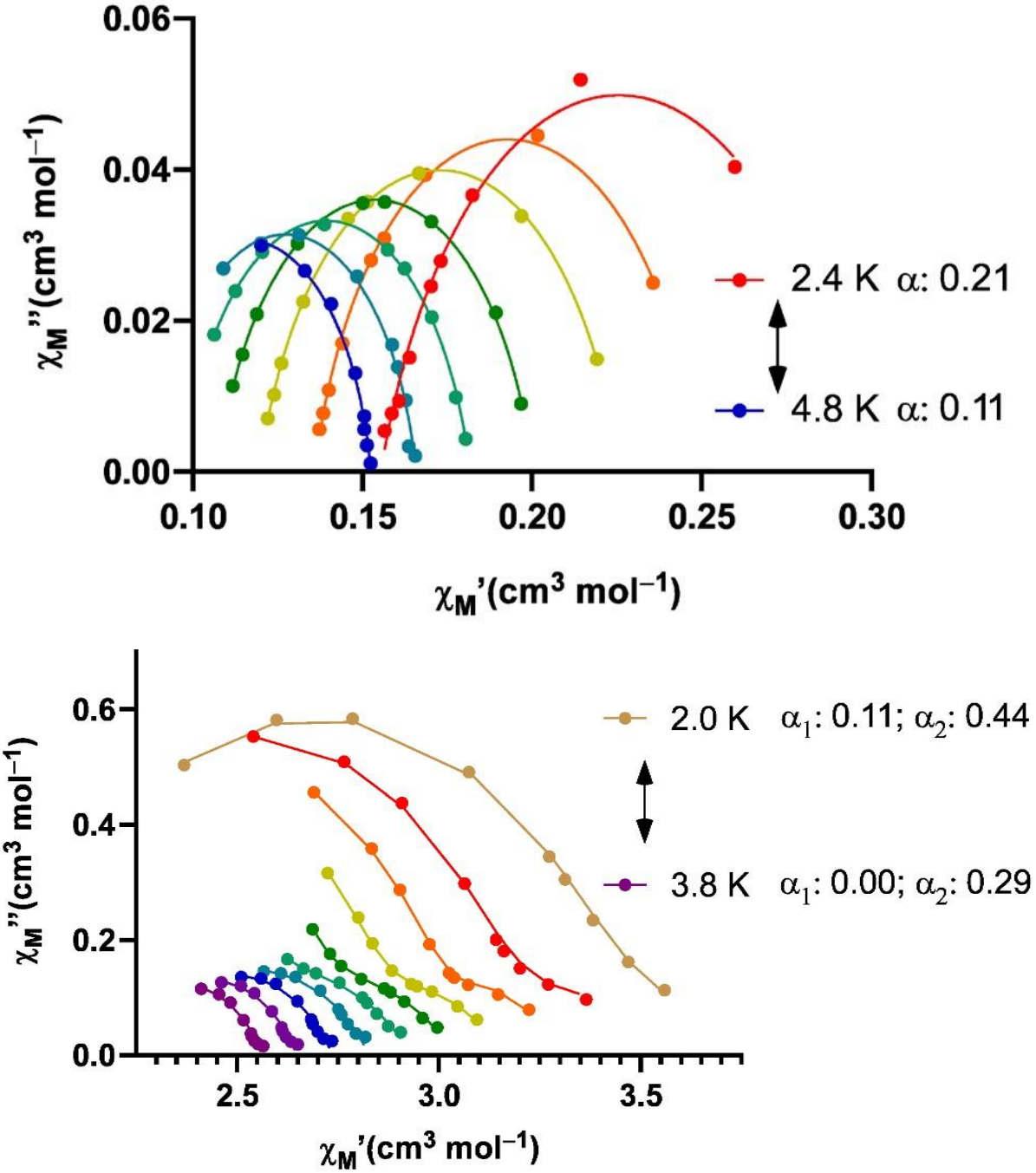

Figure S6. Cole-Cole plots in *dc* applied field of 1000 Oe for **1-Dy** (top) and **2-Dy** (bottom).

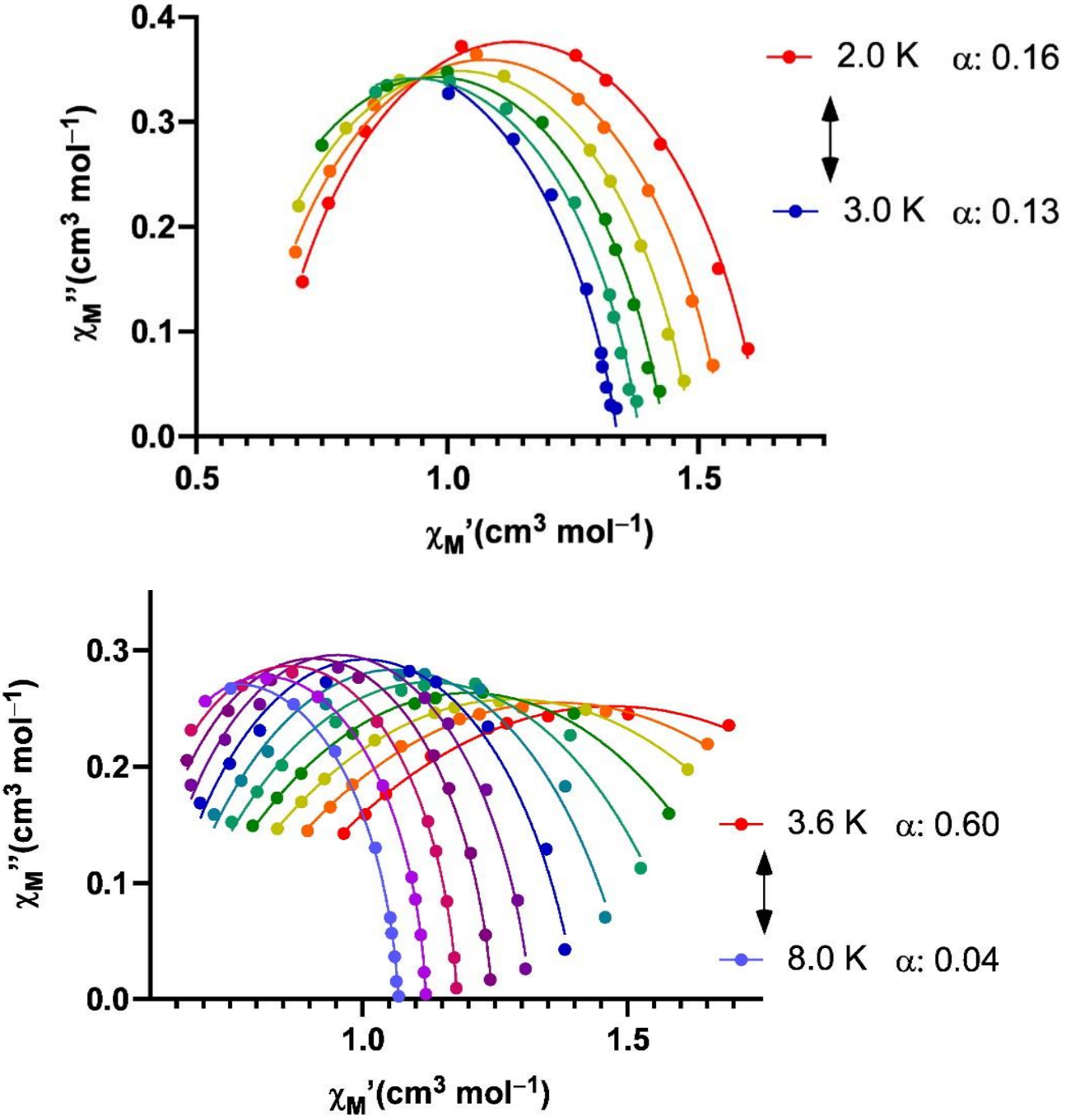

Figure S7. Cole-Cole plots in *dc* applied field of 1000 Oe for **4-Dy** (top) and **5-Dy** (bottom).

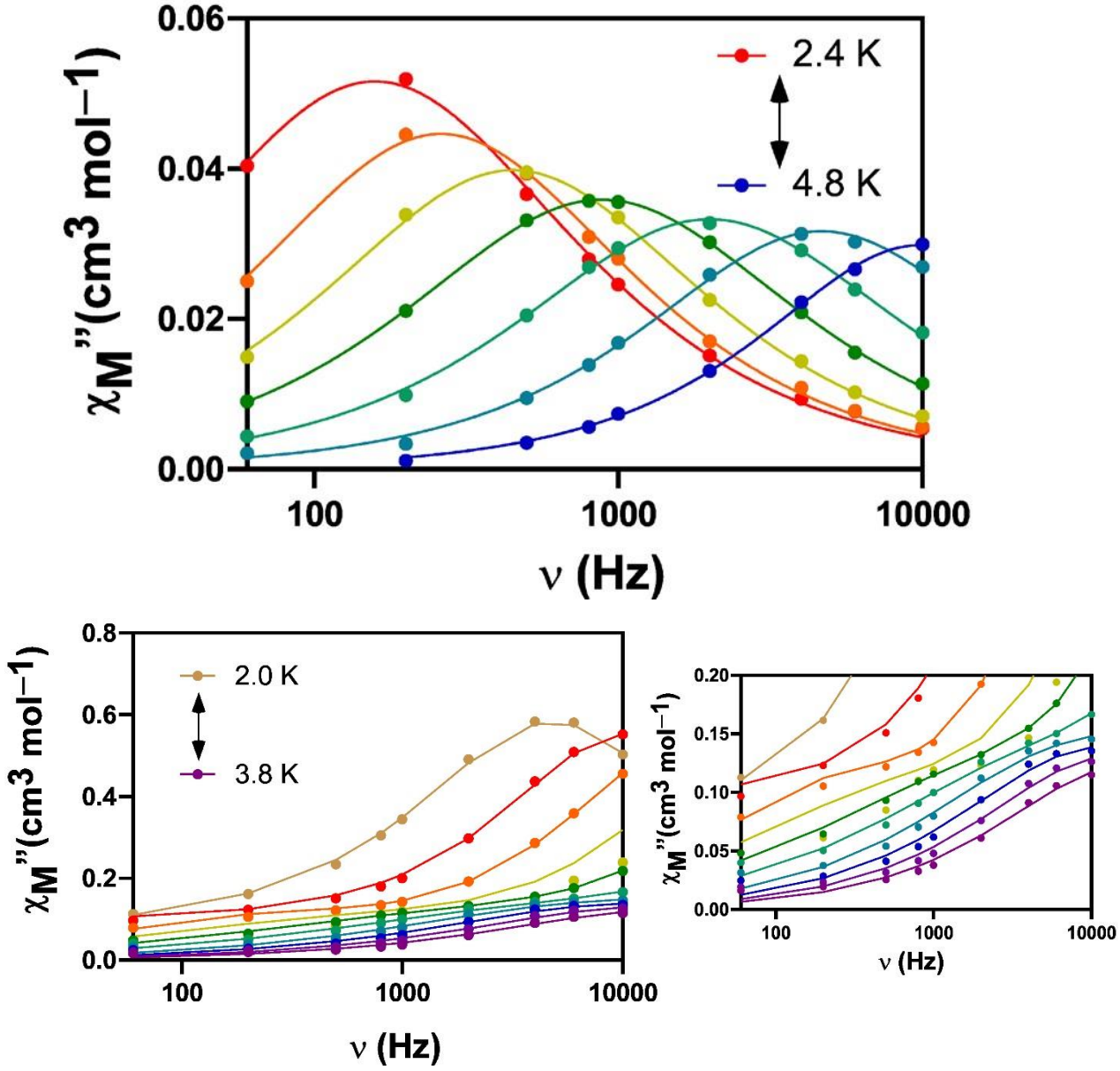

Figure S8. Variable-temperature frequency dependence of the χ_M'' signal under 1000 Oe applied field of **1-Dy** (top) and **2-Dy** (bottom).

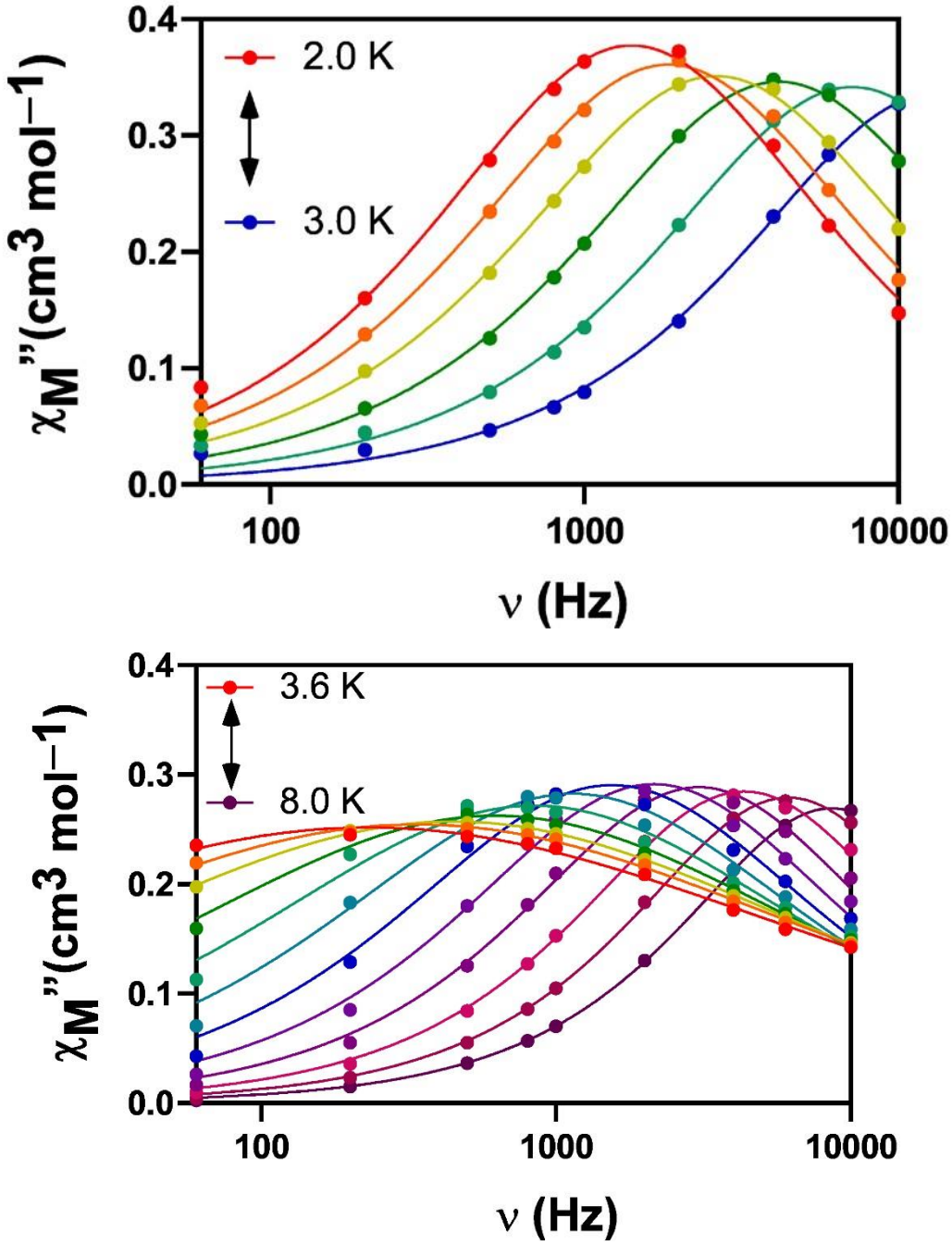

Figure S9. Variable-temperature frequency dependence of the χ_M'' signal under 1000 Oe applied field of **4-Dy** (top) and **5-Dy** (bottom).

Table S4. Relaxation Fitting Parameters from Least-Squares Fitting of χ(ϕ) data for compound **2-Dy**.

T (K)	FR		SR	
	α1	**τ1**	**α2**	**τ2**
2	0.14	3.29E-05	-	-
2.2	0.06	1.54E-05	-	-
2.4	0.13	7.28E-06	-	-
2.6	0.09	4.01E-06	0.49	2.97E-04
2.8	-	-	0.44	8.38E-05
3.0	-	-	0.42	3.59E-05
3.2	-	-	0.36	2.25E-05
3.4	-	-	0.34	1.37E-05
3.6	-	-	0.31	1.15E-05
3.8	-	-	0.29	9.34E-06

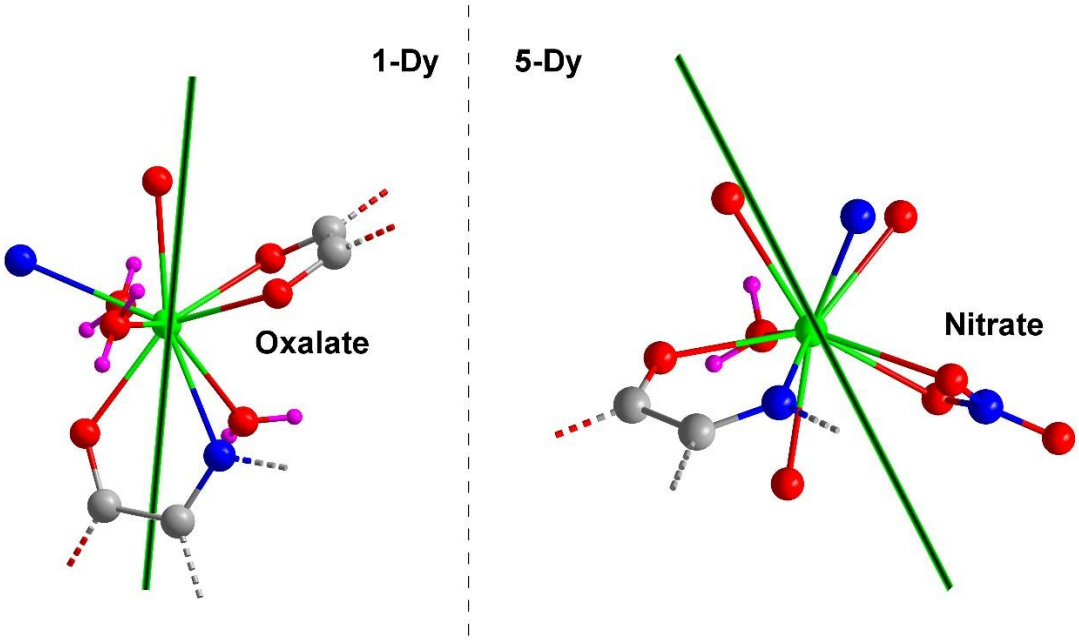

Figure S10. Theoretical orientation of the magnetic moments for Dy(III) ions in compounds **1-Dy** and **5-Dy**.

S6. Photoluminescence measurements.

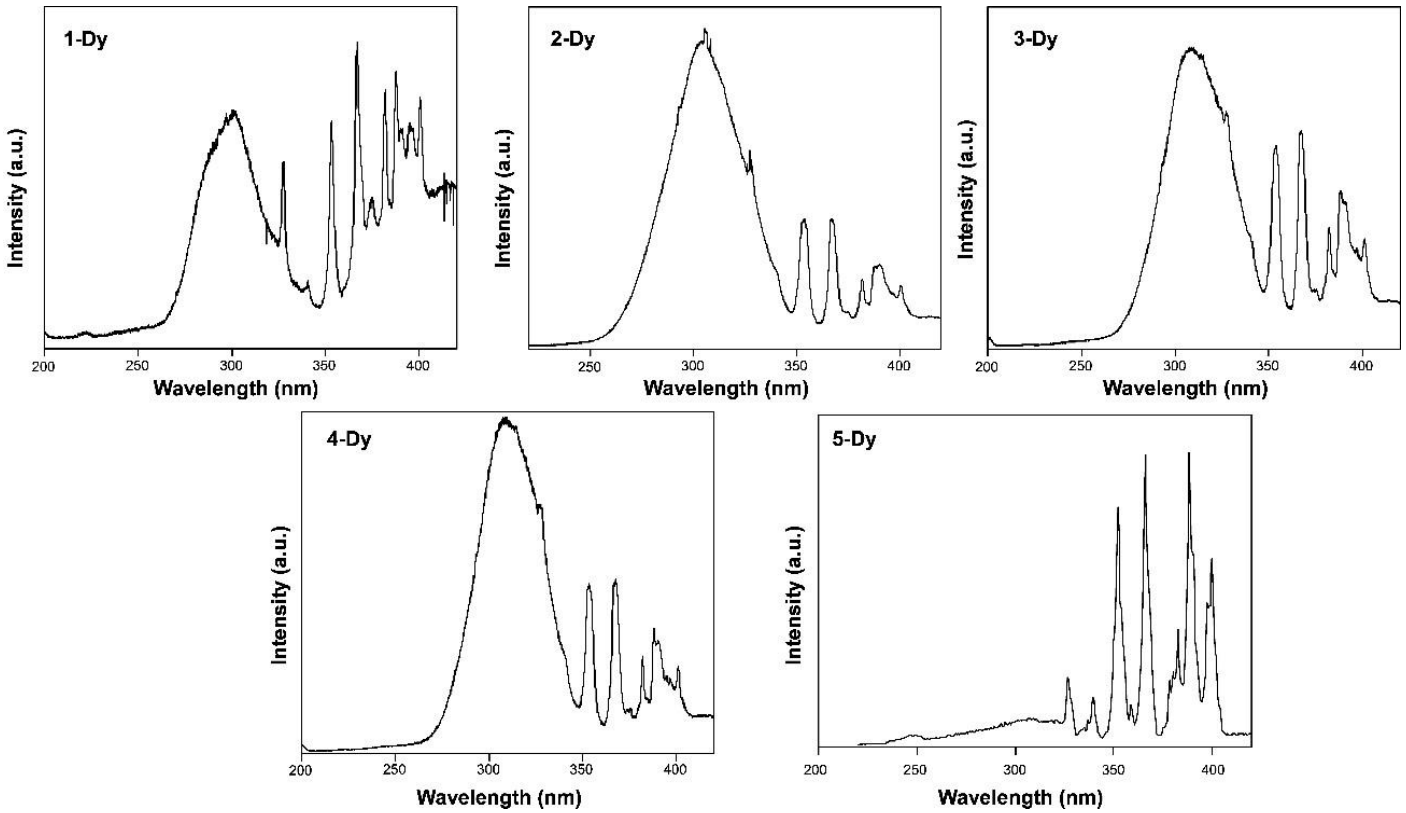

Figure S11. Excitation spectra monitored at 573 nm for compounds **1-Dy**, **2-Dy**, **3-Dy**, **4-Dy** and **5-Dy**.

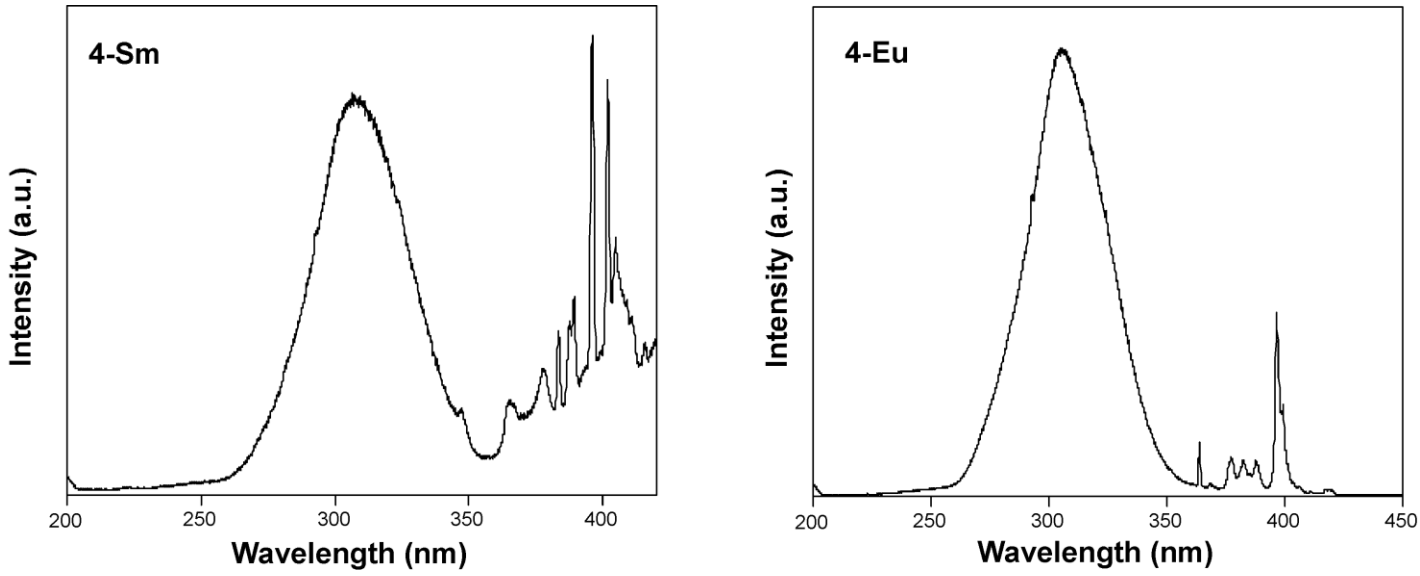

Figure S12. Excitation spectra monitored at 596 nm for **4-Sm** and at 618 nm for **4-Eu**.

S7. Luminescence lifetime measurements.

Lifetime measurements were performed at room temperature using polycrystalline samples under excitation at 325 nm for the main emission wavelengths arising from intraionic lanthanide transitions. The decay curves were recorded employing different exposure times in order to achieve 10^4 counts in the pulse of. The curves were analyzed by tail fitting. Decay curves are characterized by two distinguishable regions: i) the first rapid decreases at very short times which are associated with the pulse of the lamp and ii) the following slower decrease corresponding to the lifetime of the sample. Accordingly, the fittings show these two contributions.

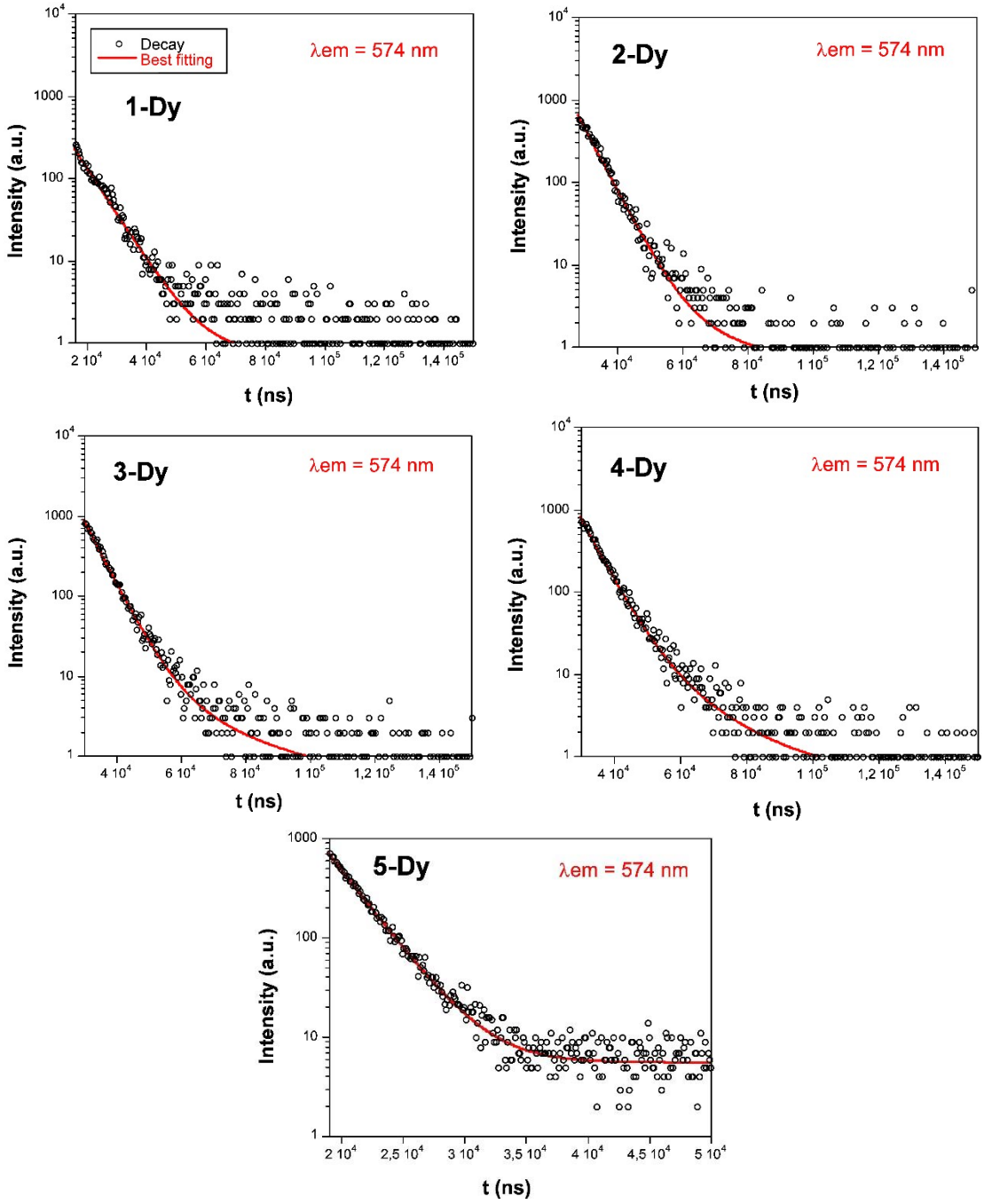

Figure S13. Emission decay curves for compounds **1-Dy**, **2-Dy**, **3-Dy**, **4-Dy** and **5-Dy** under 325 nm excitation laser showing the best fitting.

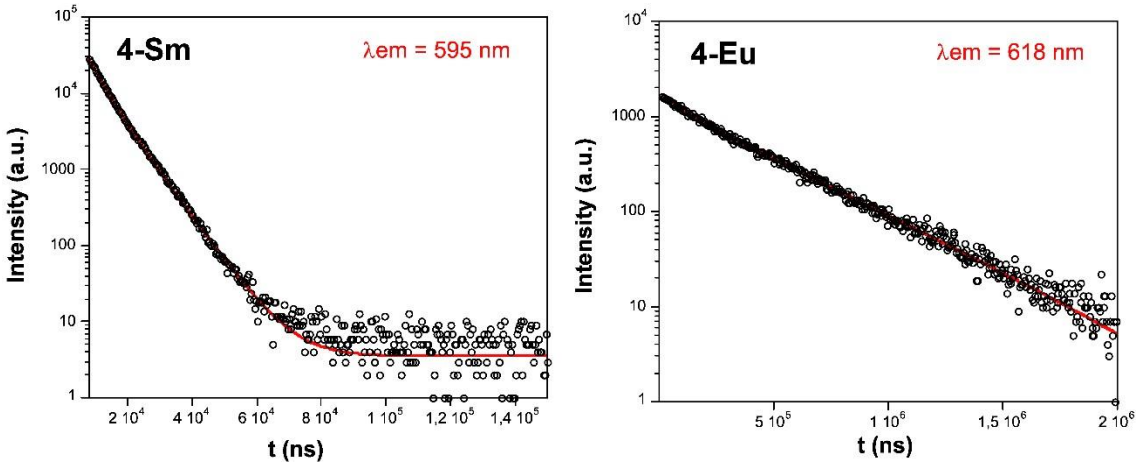

Figure 14. Emission decay curves for compounds **4-Sm** and **4-Eu** under 308 nm excitation laser showing the best fitting.

S8. Calculations of the pmdc triplet state.

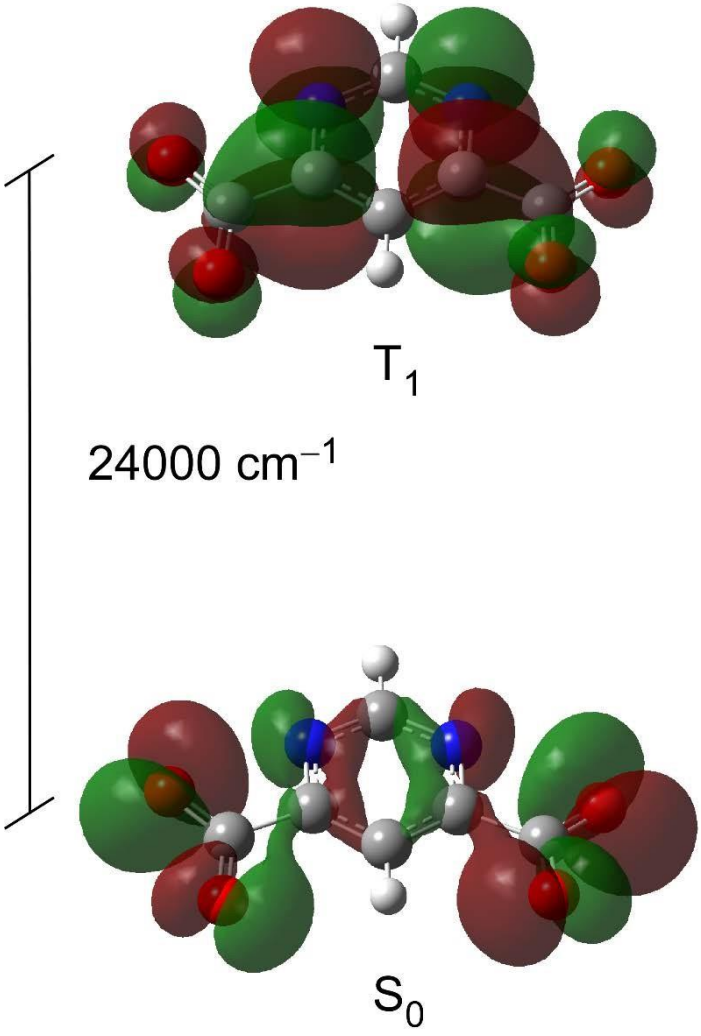

Figure S15. Illustration of the triplet and ground single state of pmdc ligand with the energy gap between them.

S9. FT-IR spectroscopy

In the following figure, the FTIR spectra of previously novel **4-Nd**, **4-Sm**, **4-Eu** and **4-Dy** compounds are described.

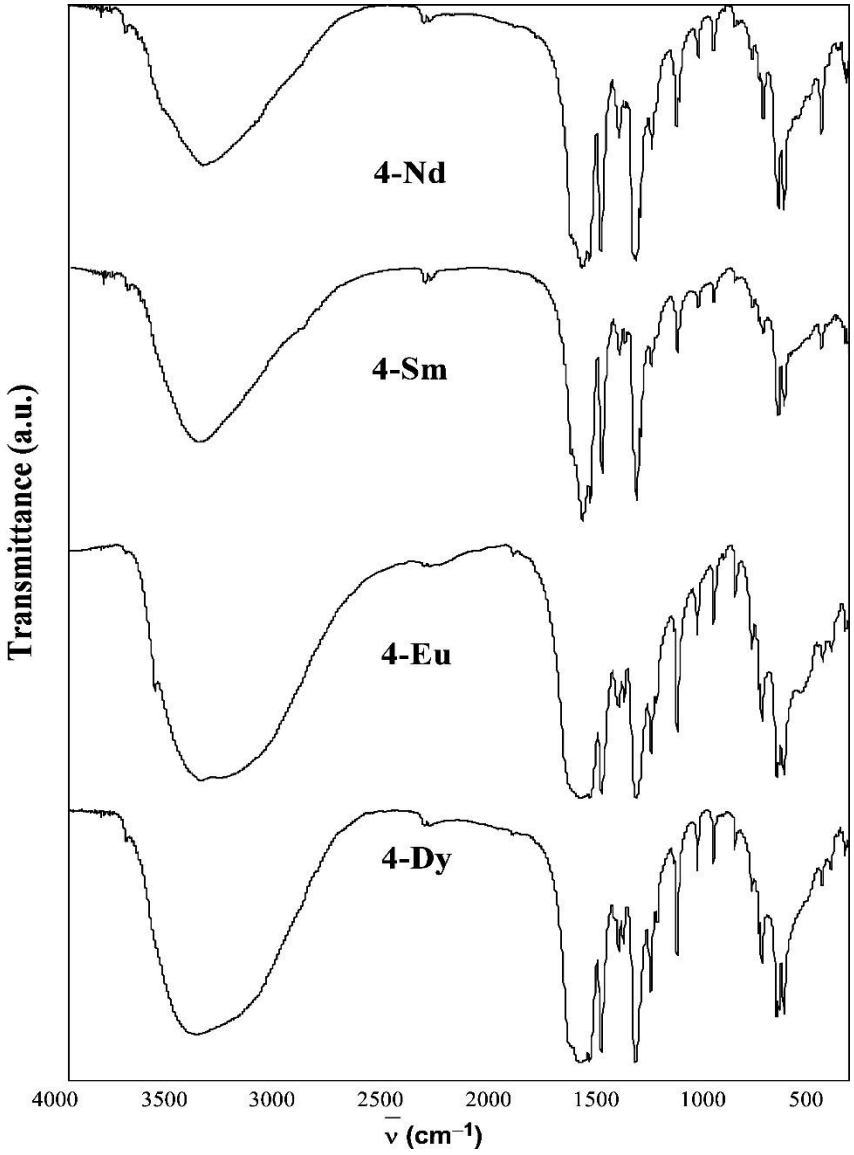

Figure S16. IR spectra of 4-Nd, 4-Sm, 4-Eu and 4-Dy.

Note that the rest of Dy-based compounds are shown in Figure S2 and can be found also in the ESI file of the corresponding publication[1].

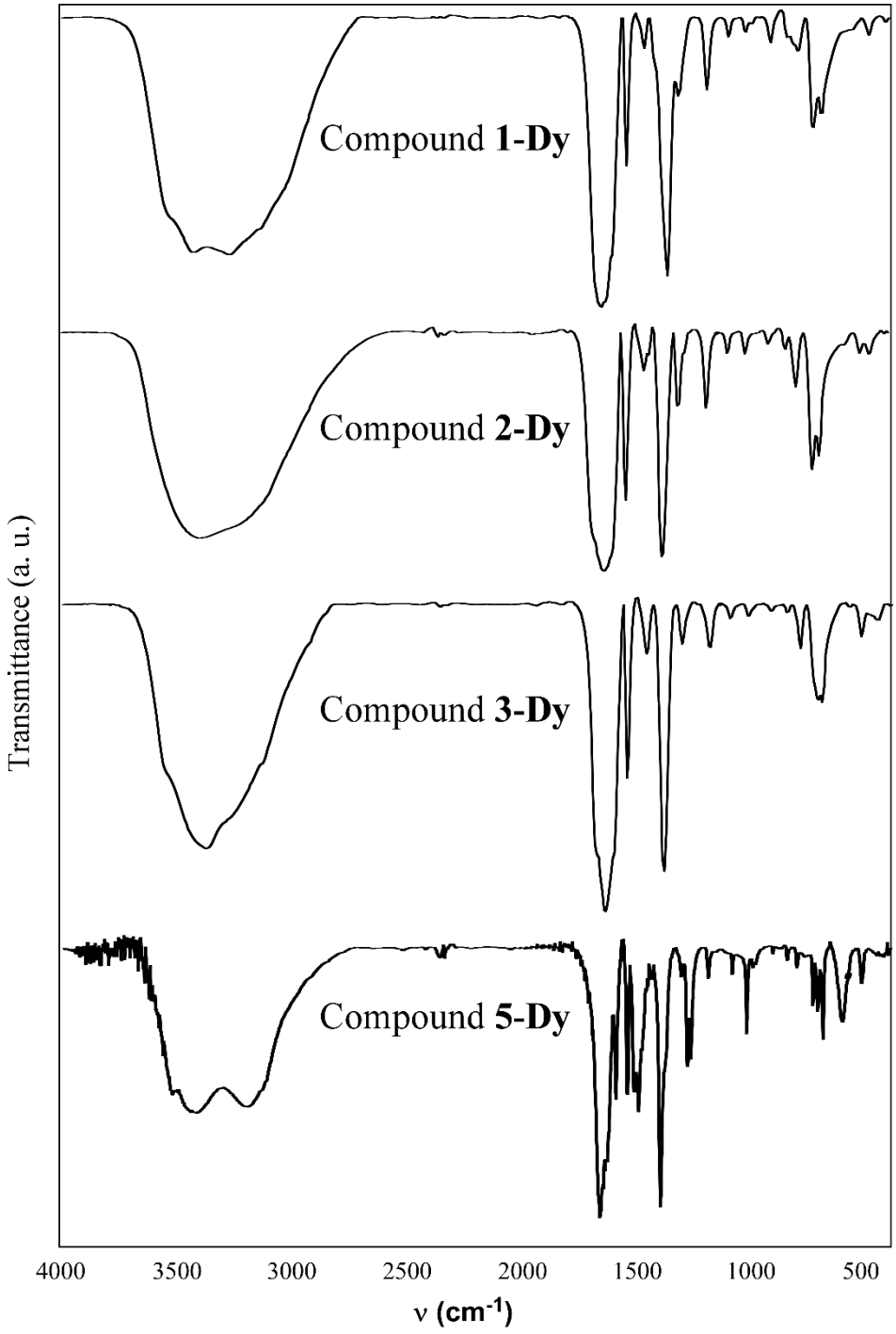

Figure S17. FTIR spectra of all Dy-based compounds.

[1](a) Cepeda, J.; Balda, R.; Beobide, G.; Castillo, O.; Fernández, J.; Luque, A.; Pérez-Yáñez, S.; Román, P.; Vallejo-Sánchez, D. Lanthanide(III)/Pyrimidine-4,6-dicarboxylate/Oxalate Extended Frameworks: A Detailed Study Based on the Lanthanide Contraction and Temperature Effects. Inorg. Chem. **2011**, 50, 8437–8451. (b) Cepeda, J.; Pérez-Yáñez, S.; Beobide, G.; Castillo, O.; García, J.A.; Lanchas, M.; Luque, A. Enhancing

luminescence properties of lanthanide(III)/pyrimidine-4,6-dicarboxylato system by solventfree approach. Dalt. Trans. **2015**, 44, 6972–6986.